An experimental facility for latent heat thermal energy storage units

Hector Bastida[1], Amanda Younes[1,2], Carlos E. Ugalde-Loo[1], Rob Smart[2], Mansoureh Khaljani[1,2], Nick Jenkins[1], Babar Baluch[2]
[1]School of Engineering, Cardiff University, Cardiff, Wales, United Kingdom
[2]SRS Works Ltd, Berkshire, England, United Kingdom
{BastidaHernandezJH@cardiff.ac.uk, YounesA@cardiff.ac.uk, Ugalde-LooC@cardiff.ac.uk, Robert.Smart@srsworks.co.uk, KhaljaniM@cardiff.ac.uk, JenkinsN6@cardiff.ac.uk, Babar@srsworks.co.uk}

***Abstract*—Assessing the performance of thermal energy storage (TES) units beyond software simulation requires testing in a controlled environment, with specific operating modes, and in safe conditions. A test-rig with an energy source and a monitoring system is very helpful to conduct experimental tests to assess the performance of TES systems. To this end, this paper presents an experimental facility for the study of latent heat TES (LH-TES) units. Emphasis is placed on the individual elements of the facility, which includes plumbing components and electric heaters to support the charging process of the TES units. Water is used as the heat transfer fluid (HTF). To demonstrate the capabilities of the test-rig, an LH-TES prototype for heating applications is used. Four different configurations and three operating modes are assessed: charging, discharging and discharging-mixing. The wide range of the experiments possible with the developed facility enables testing of early designs of LH-TES units ahead of deployment in real thermal networks.**

Keywords—Thermal energy storage, phase change material, latent heat, test rig.

I. Introduction

Reducing greenhouse emissions is critical for all sectors involved in the generation, supply and consumption of energy. The change in energy consumption habits and the incorporation of renewable energy sources into the residential sector shows the active role that consumers may play in achieving net-zero greenhouse emissions targets set by, for example, the UK Government [1], [2]. This is also facilitated by the inclusion of thermal energy storage (TES) systems.

The use of TES systems in residential buildings and houses has increased considerably [3]–[5], with hot water tanks (HWTs) being the most common option for storing heat. HWTs rely on sensible heat. However, phase change materials (PCMs) have high latent heat values, which enables them to store a substantial amount of heat within a small volume. A latent heat TES (LH-TES) unit requires less space compared to a HWT to store a similar amount of heat and, therefore, represents a more space efficient option for heat storage in the residential sector.

Substantial research on different types of PCMs for hot and cold stores is available in the literature [6], [7]. For instance, the use of paraffin wax has been reported several years ago [8], [9]. New types of PCM with improved thermophysical properties (e.g. specific heat and thermal conductivity) to increase the energy storage capacity have also been presented [10]–[12]. However, a typical drawback of PCMs, besides the toxicity of some materials, is their low thermal conductivity. This gives a limited heat transfer capability during the charging and discharging processes of LH-TES units. Some solutions have been proposed in the literature. For instance, different internal structures of the TES units with an increased heat transfer area or with improved hydraulic conditions of the heat transfer fluid (HTF) have been presented [13], [14]. The inclusion of fins with a high thermal conductivity has also been studied [15].

To assess the enhancements brought by the previous options, mathematical models are employed [16]. However, the accuracy of simplified models or the large computing time required to simulate very detailed models are limitations when analyzing the performance of LH-TES units. A way to complement simulation-based analysis is by conducting experimental work. The use of experimental facilities has been reported in the literature [17], [18]. However, sufficient information on the test-rig is often omitted as the focus of the work is usually not the experimental facility itself. In other cases, the operating modes to carry out the experiments are not explained in detail [19], [20].

This paper presents an experimental test-rig for heating applications suitable for assessing the performance of LH-TES units. Emphasis is placed on the test-rig and its main components. To demonstrate the capabilities of the facility, four TES unit configurations and three operating modes are considered: charging, discharging, and discharging-mixing. The discharging-mixing is an innovative set-up where the output of the TES unit is blended with cold water to extend the time of hot fluid provision at a constant temperature.

The experimental facility is flexible and able to analyze different configurations of TES units for domestic heating applications employing water as the HTF. However, other fluids such as glycol mixtures may be adopted to improve heat transfer during discharging and charging processes [21], [22]. The test-rig allows experiments to be undertaken in a safe way, the impact of hydraulic and thermal conditions (e.g. different temperatures and volumetric flows) to be assessed over a TES unit, and practical operating conditions of a thermal system to be emulated without compromising its operation. The wide range of the possible experiments enables early designs of LH-TES units to be tested ahead of deployment in real thermal networks.

II. The Experimental Facility

A schematic of the experimental facility is shown in Fig. 1. It consists of the LH-TES unit, a pump, a heater system, a mixing valve, and sensors for volumetric flow and temperature. To reduce the pressure of the HTF that flows through the system, a pressure reducer is included.

The experimental facility is divided into four main components, which are shown in Fig. 2: the LH-TES unit, instrumentation, heat supply, and plumbing (pump, pipes, and valves).

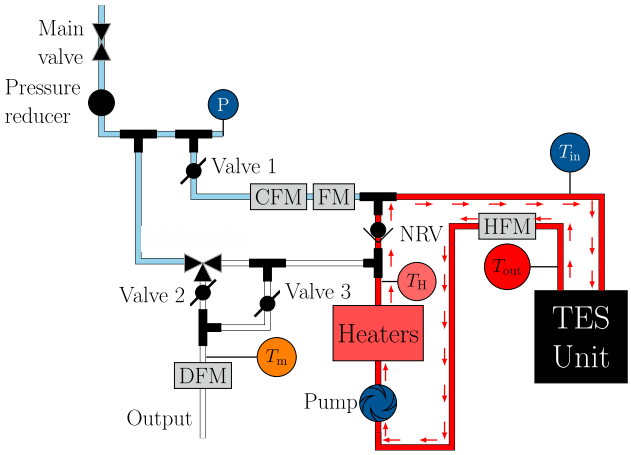

Fig. 1. Schematic of the experimental facility (charging process).

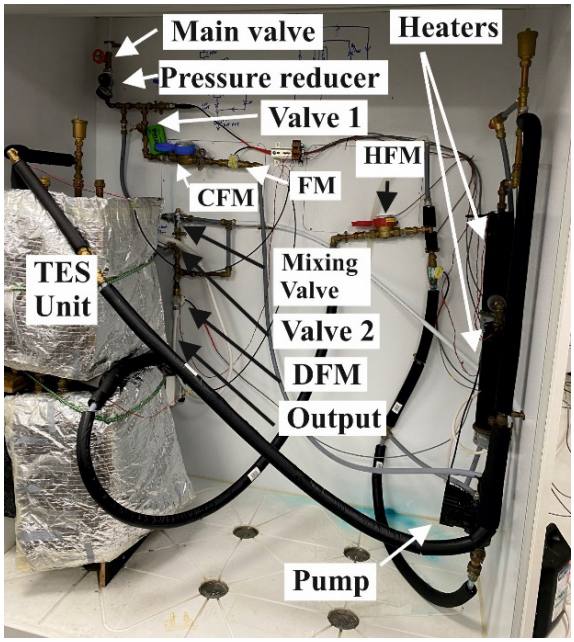

Fig. 2. Main components of the experimental facility.

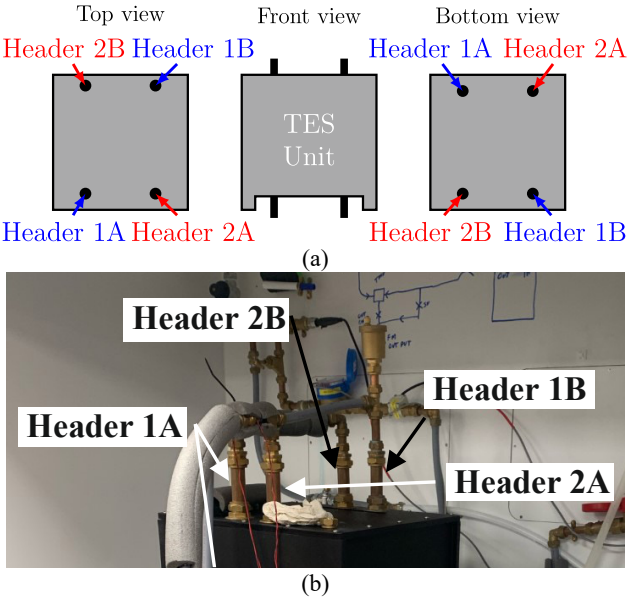

Fig. 3. LH-TES unit's headers: (a) schematic of top, front and bottom views; (b) photo and schematic of the TES unit's headers.

A. *LH-TES unit*

The LH-TES unit comprises two heat exchangers submerged in a PCM [23]. The HTF (i.e. water) circulates through the channels of the heat exchangers to supply and remove heat from the PCM by convection and conduction heat transfer. The heat exchangers are connected at their ends A and B through a vertical header, as shown in Fig. 3. This enables different configurations for testing.

B. *Instrumentation*

The thermal performance of the TES unit is monitored using three temperature sensors (model DS18B20) [24] to capture the input and output temperatures of the HTF (T_{in} and T_{out}) and the temperature after the mixing valve (T_m).

Volumetric flow sensors are installed to measure the flow of the HTF in four different locations of the system. A pressure sensor is located after the pressure reducer to indicate the input pressure of the HTF. Also after the pressure reducer, the flow through the pipes is monitored using an analogue flow meter (CFM) [25] and a digital flow meter (FM). The volumetric flow during discharging processes is recorded with a digital flow meter (HFM) as well as the output flow of the system (DFM). The three flow meters are similar (YF-S201 model by UKUR [26]).

C. *Heat Supply*

The HTF is heated using two heaters connected in series, each with a power rating of 3 kW [27]. The HTF flows through the heaters, where an electric resistance is used to increase the temperature of the HTF up to 80°C.

The experimental facility regulates the temperature of the charging process to ensure repeatability in testing. For this purpose, a temperature feedback control loop is implemented (see Fig. 4). A digital thermometer is located immediately after the heaters. An on/off controller within the monitoring system activates a relay ('smart switch') which, in turn, regulates the on/off switching of the heaters [28]. The monitoring system quantifies the power supplied by the heaters considering the time that the 'smart switch' is on.

D. *Plumbing*

A pump [29] is used to circulate the HTF in the system during charging and discharging processes. The pipes connecting the system components are made of cross-linked polyethylene, which is adequate for high HTF temperatures [30]. To avoid heat losses after the HTF is heated, the pipes within the charging loop and the pipe that connects the heaters to the mixing valve are covered by Noma rubber foam pipe lagging [31]. The mixing valve is used to blend water coming from the TES unit with cold water to achieve reference set-point temperatures during discharging-mixing processes. The mixing valve offers a temperature range of 38°-46°C, which is adequate for residential applications [32].

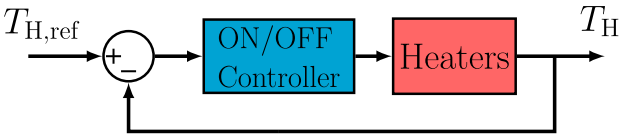

Fig. 4. Block diagram of the temperature control for the heaters.

III. Case Studies

To demonstrate the capabilities of the experimental facilities, the performance of the LH-TES unit was investigated under three operating modes: charging, discharging and discharging-mixing. For all modes, different set-points of the HTF's volumetric flow rate and the charging temperature are possible.

A. LH-TES Unit Configurations

The LH-TES unit used can be reconfigured by connecting the heat exchangers either in parallel or in series. Thus, the headers of the heat exchangers can be switched from input to output depending on the selected connection.

Fig. 5 shows the four configurations tested. The first two options (*a* and *b*) connect heat exchangers 1 and 2 in series. This means that the output of heat exchanger 1 (header 1B) is linked to the input of heat exchanger 2 (header 2A)—see Fig. 3. The overall input of this arrangement is header A of heat exchanger 1, while the output is header B of heat exchanger 2. The main difference between the two series configurations is in the locations of the input and output of the HTF: bottom in option *a*, and top in option *b*. The ends of the headers not used are blocked.

For the parallel configurations, headers 1A and 1B are connected (see Fig. 3), so the input of the HTF is split into both heat exchangers. The output of the unit is given by the link between headers 2A and 2B. The difference between the arrangements *c* and *d* is in the location of the input: top and bottom, respectively.

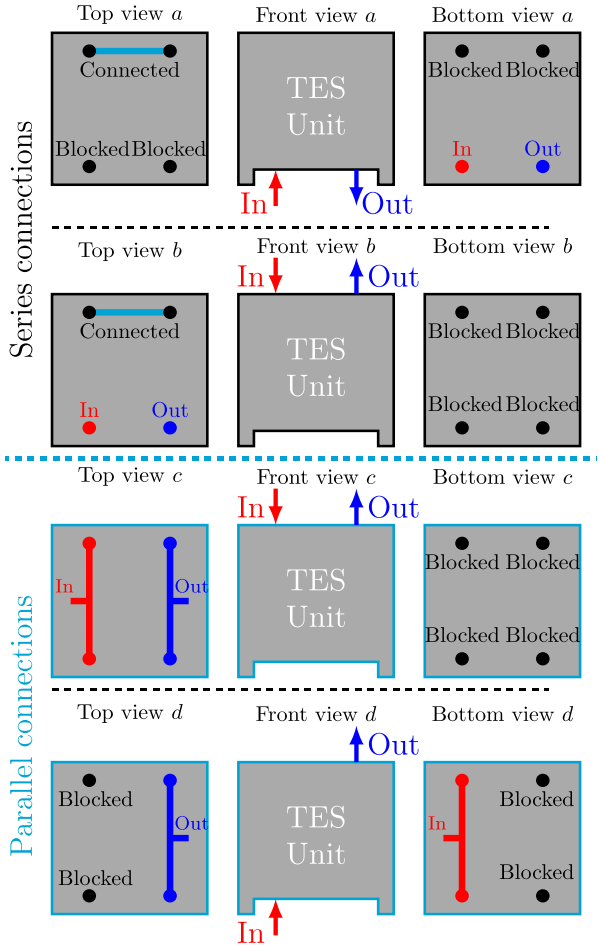

Fig. 5. Heat exchanger set arrangements of the TES unit: *a* and *b* in series and *c* and *d* in parallel.

B. Charging Process

Fig. 1 presents a schematic of the charging process. A hydraulic loop is created by closing valves 2 and 3 and turning on the pump. A non-return valve (NRV) stops any backflow. The set-point of the pump is modified according to the required volumetric flow. The pressure generated by the pump forces the HTF to recirculate through a loop as shown by the red arrows. Then, the heaters are turned on to gradually increase the temperature of the HTF to 75°C.

Three main variables are monitored: volumetric flow rate, temperature, and power. The input and output temperatures of the HTF inside the TES unit are used to quantify the duration of the charging process. A complete charge is assumed when the output temperature meets the set-point of the heater's temperature controller.

Volumetric flow rate is a key variable in the performance of the unit as it is directly related to the heat transfer between the HTF and the PCM. Variations in volumetric flow thus affect the duration of charging. It is also used to calculate the thermal power P_{Th} [W] provided by the HTF with

$$P_{\mathrm{Th}} = \dot{m}_{\mathrm{HTF}}(T_{\mathrm{out}} - T_{\mathrm{in}}), \qquad (1)$$

where $\dot{m}_{\mathrm{HTF}}$ [kg/s] is the mass flow rate of the HTF, V_f [l/min] its volumetric flow ($\dot{m}_{\mathrm{HTF}} = V_f/3600$), T_{out} [°C] its output temperature, and T_{in} [°C] its input temperature.

To assess the efficiency of the charging process, tests were conducted to compare the thermal energy absorbed by the TES unit against the electrical energy provided by the heaters. Fig. 6 shows the charging process of configuration *a* at a volumetric flow of 7.7 l/min (top plot). The input and output temperatures (T_{in} and T_{out}) of the HTF increase gradually to 75°C from an initial condition of 22°C (middle plots). The slope of curve T_{out} is nearly zero between 53°C and 58°C, which indicates the PCM is changing phase from solid to liquid and absorbs latent heat. Since there are no internal sensors monitoring the PCM, it is assumed that melting is complete once T_{out} >58°C. This means that the total latent heat is stored in approximately 23 minutes. However, additional energy is added as sensible heat to ensure a complete phase transition of the PCM.

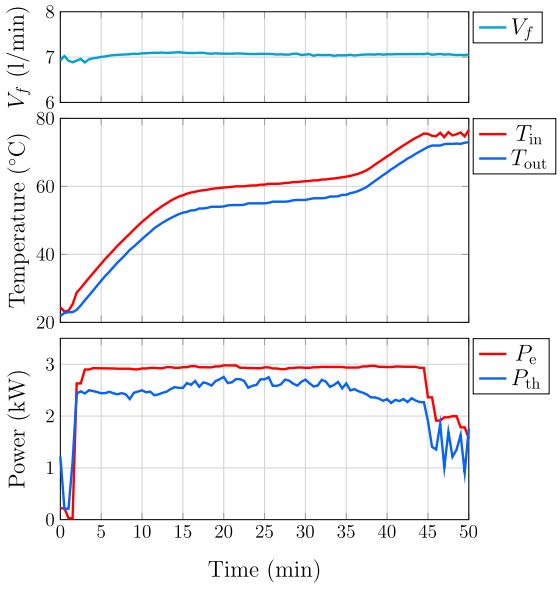

Fig. 6. Experimental results. Charging process for configuration *a*: Volumetric flow (top), input and output temperatures of HTF (middle) and the electrical and thermal power (bottom).

Fig. 6 (bottom plot) also shows the electrical power P_e provided by the heaters and the thermal power P_{th} calculated with (1). Electrical and thermal energy (kWh) are quantified by integrating the power curves. In this case, the total electrical energy supplied by the heaters is 2.06 kWh and the total thermal energy absorbed by the PCM is 1.79 kWh. This represents an efficiency of 86% for the charging process.

Fig. 7 shows experimental results of the charging process at different volumetric flows for the four configurations. For clarity, only the output temperature of the HTF is provided. Subscripts *a*, *b*, *c* and *d* stand for the configurations shown in Fig. 5. The transition zone where the PCM melts starts approximately 12 minutes after initiating the test and lasts for 23 minutes. Due to the gradual increment of the input temperature, the duration of the process is not affected by the heat exchanger configuration, or by the volumetric flow of the HTF. Thus, the only way to accelerate charging is by increasing the input temperature of the HTF at a faster rate. This could be achieved by increasing the power of the heaters (although doing this is out of the scope of this work).

C. Discharging Process

Fig. 8 presents a schematic of the discharging process. The heaters and the pump are turned off. Valve 2 is closed, whereas valve 1 and outlet valve 3 are opened. The NRV ensures the incoming HTF flows through the TES unit to exit the system. Thus, discharging considers only the direct output of the TES unit. The flow of the HTF is provided only by the pressure given by the pressure reducer. Manual regulation of valve 1 modifies the volumetric flow of the HTF.

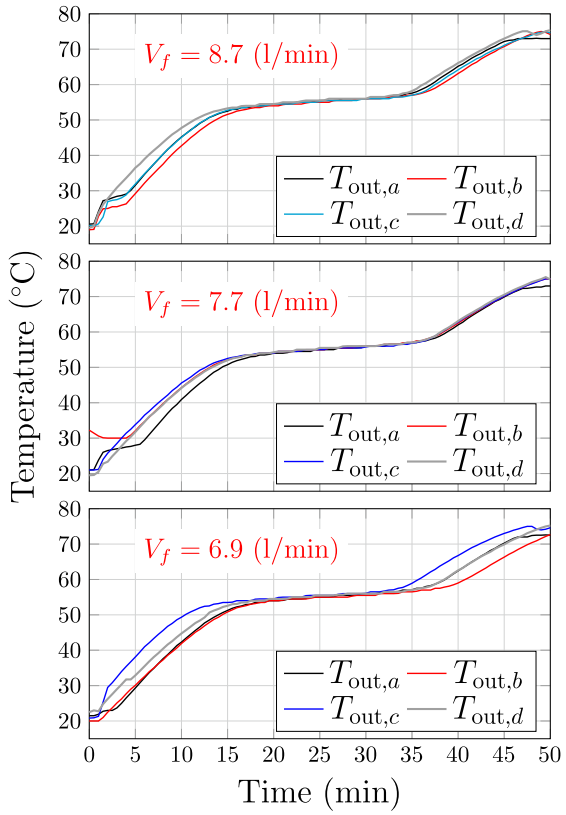

Fig. 7. Output temperature of the HTF for the four configurations of the LH-TES unit (see Fig. 5) during charging at different volumetric flows: 8.7 l/min (top), 7.7 l/min (middle) and 6.9 l/min (bottom).

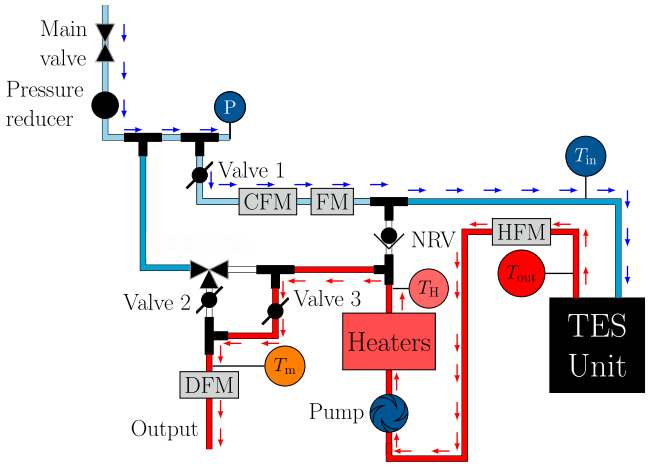

Fig. 8. Schematic of the discharging process.

Fig. 9 shows the results of a discharging process for configuration *a* with a volumetric flow of 7.4 l/min (top plot). The HTF flows through the unit taking out the heat from the PCM. At the beginning of the process, the output temperature of the HTF is at 70°C (T_{out}). Then, as the heat stored in the PCM starts running out, T_{out} decreases to 20°C (middle plot) to match the input temperature of the HTF (T_{in}). The amount of thermal power is quantified using (1) and the total energy transferred is calculated by integrating the power curve as in the charging process. The total thermal energy provided by the LH-TES unit is 1.61 kWh, which represents an efficiency of 78% for the discharging process.

The criteria used to define a full discharge may vary depending on the output temperature of the HTF. The TES unit is considered totally discharged when this temperature is approximately 25°C. This value is near the end of the total exothermic process of the PCM according to its differential scanning calorimetry diagram given in [23]. This means that the latent heat has been fully released.

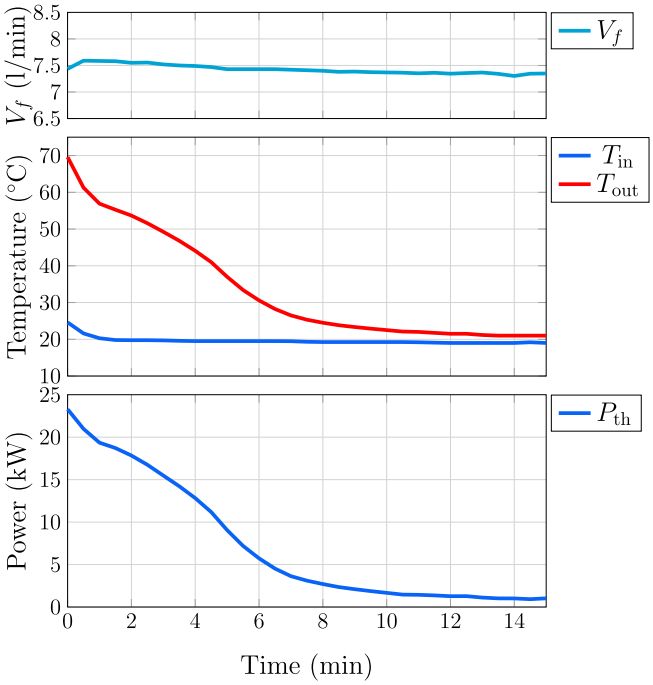

Fig. 9. Experimental results. Discharging process for configuration a: volumetric flow (top), input and output temperatures of the HTF (middle) and thermal power released (bottom).

Experimental results of the discharging process at different volumetric flows for the four configurations are shown in the Fig. 10. The input temperature of the HTF for all tests is about 20°C. As opposed to the charging process, the volumetric flow significantly affects the duration of discharging. In this case, the larger the volumetric flow of the HTF at a constant temperature is, the faster the heat transfer between the HTF and the PCM becomes. A complete discharge of the unit for 7.4, 4.2 and 2.0 l/min is achieved in 10, 17 and 43 minutes, respectively.

The discharging performance is similar for medium and high flows regardless of the unit configuration. However, slight differences are noticeable between the series (*a* and *b*) and parallel (*c* and *d*) configurations at low volumetric flows. Focusing on the bottom plots of Fig. 10, during the phase change of the PCM, the HTF for parallel configurations exhibits a higher output temperature than for the series arrangements. There is a temperature difference of ~3°C. Although this is small, it implies that parallel configurations have a slightly better discharging performance.

D. Discharging-mixing process

The third operating mode includes a mixing valve to assess the performance of the LH-TES unit when hot HTF is mixed with cold water from the system input to achieve a temperature set-point. Such an operating condition resembles a real implementation of TES systems (e.g. 'cold' tap water could be at 10°C during winter). Fig. 11 shows the direction of the HTF flow through the system during the discharging-mixing process. Valve 1 is open at 100%, valve 3 is closed and valve 2 is used to establish the desired volumetric flow at the system output (orange arrows) by adjusting its opening.

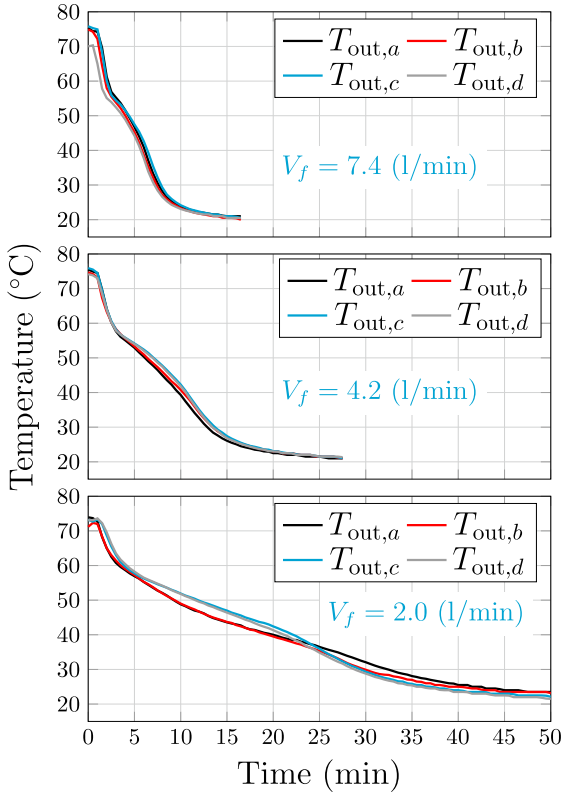

Fig. 10. Output temperature of the HTF for the four configurations (see Fig. 5) during discharging at different volumetric flows: 7.4 l/min (top), 4.2 l/min (middle) and 2.0 l/min (bottom).

The mixing valve has a thermostat that internally modifies the volumetric flow of the incoming fluid to achieve a desired reference temperature. In Fig. 11, cold water is shown with blue arrows and the HTF with red arrows. The discharging-mixing process can be analyzed by increasing the flow through the TES unit. To this end, the pump is switched on to increase the pressure and to ensure sufficient flow. This improves the heat transfer between the HTF and the PCM.

As LH-TES unit configurations with parallel connections (*c* and *d*) presented a better performance for the discharging process, configuration *c* (see Fig. 5) is adopted to carry out two discharging-mixing tests. Two volumetric flows (3.5 and 5 l/min) and a temperature reference of 40°C ($T_{m,r}$) are used. The value of $T_{m,r}$ is adjusted with the mixing valve.

Fig. 12 shows the experimental results. The volumetric flows of the cold water (V_t), HTF (V_f), and the mixing valve output (V_m) are shown in the top plots. V_t and V_f are regulated to achieve the desired $T_{\mathrm{m,r}}$ (bottom plots). The volumetric flow of the HTF starts to increase when its temperature decreases, which coincides with a decrement in volumetric flow of the cold water. Although slight variations in V_m are exhibited, its value remains close to that adjusted by valve 2.

The LH-TES unit can provide hot water at a constant temperature ($T_{\mathrm{m,r}}$) during 17 minutes for a volumetric flow of 3.5 l/min and during 10 minutes for 5 l/min.

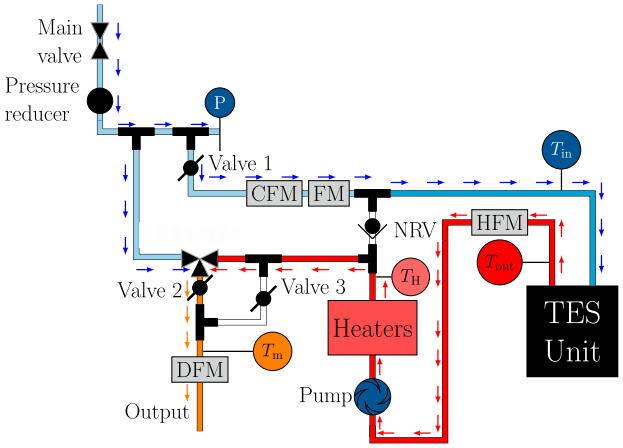

Fig. 11. Schematic of the discharging-mixing process.

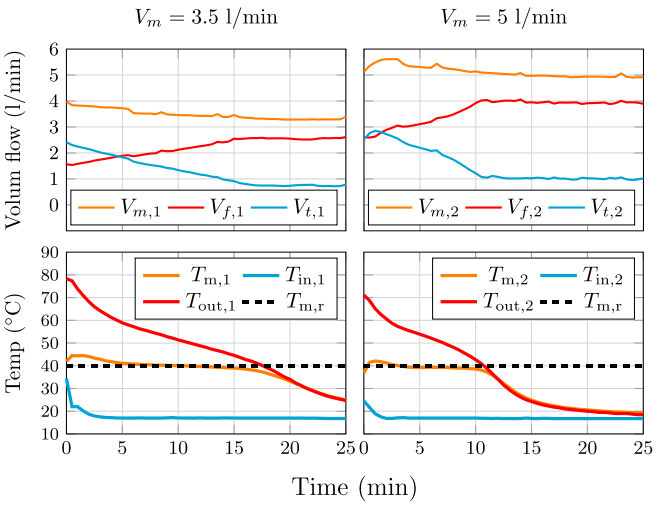

Fig. 12. Experimental results. Discharging-mixing process for configuration c: volumetric flow (top) and temperature (bottom).

Although an overshoot in the output temperature of the mixing valve occurs at the beginning of the process, the performance of the TES unit is acceptable if a tolerance of ±3°C in its output temperature is established.

IV. Conclusions

An experimental facility for the assessment of LH-TES units has been presented. The main components required to run charging and discharging processes of a TES unit have been introduced. With the facility, different hydraulic and thermal operating conditions (e.g. charging temperature, volumetric flow) can be set up to replicate operating conditions of practical implementations.

Experiments for four different TES unit configurations (two connecting the unit's heat exchangers in series and two in parallel) were analyzed under different operating modes. Results showed that performance under different volumetric flows for charging and discharging processes was similar regardless of the unit configuration. A discharging-mixing process where the HTF output is mixed with cold water to achieve a reference temperature was also analyzed. Results demonstrate the capability of the TES unit to supply hot water at a constant temperature during an extended period of time.

The case studies show the suitability of the experimental facility to assess different operating modes of a LH-TES unit under a range of hydraulic and thermal conditions. By incorporating electrical heaters with suitable temperature control, PCMs with different melting temperature may be studied. Moreover, the pump enables the study of different TES units requiring higher pressure and volumetric flows. In addition, the modular design of the test-rig enables the assessment of TES units with different shapes and sizes.

Acknowledgment

The work presented in this paper was supported by FLEXIS—part-funded by the European Regional Development Fund (ERDF), through the Welsh Government (WEFO case number 80386). This work was also supported by Innovate UK, UK Research and Innovation, through the KTP projects KTP011693 and KTP012503 and by the Engineering and Physical Sciences Research Council (EPSRC), UK Research and Innovation, through the project 'Flexibility from Cooling and Storage (Flex-Cool-Store)', Grant EP/V042505/1.

References

[1] M. Pothitou, A. J. Kolios, L. Varga, and S. Gu, 'A framework for targeting household energy savings through habitual behavioural change', *Int. J. Sustain. Energy*, vol. 35, no. 7, pp. 686–700, Aug. 2016.

[2] *Net Zero Strategy: Build Back Greener*, Great Britain, HM Government, Department for Business, Energy and Industrial Strategy 2021.

[3] B. Zalba, J. M. Marín, L. F. Cabeza, and H. Mehling, 'Review on thermal energy storage with phase change: materials, heat transfer analysis and applications', *Appl. Therm. Eng.*, vol. 23, no. 3, pp. 251–283, Feb. 2003.

[4] D. Boer, *et al.*, 'Approach for the analysis of TES technologies aiming towards a circular economy: Case study of building-like cubicles', *Renew. Energy*, vol. 150, pp. 589–597, May 2020.

[5] L. F. Cabeza, *et al.*, 'Perspectives on thermal energy storage research', *Energy*, vol. 231, p. 120943, Sep. 2021.

[6] A. Tafone, *et al.*, 'Innovative cryogenic Phase Change Material (PCM) based cold thermal energy storage for Liquid Air Energy Storage (LAES) – Numerical dynamic modelling and experimental study of a packed bed unit', *Appl. Energy*, vol. 301, p. 117417, Nov. 2021.

[7] D. Vérez *et al.*, 'Experimental Study on Two PCM Macro-Encapsulation Designs in a Thermal Energy Storage Tank', *Appl. Sci.*, vol. 11, no. 13, Art. no. 13, Jan. 2021.

[8] Y. Li and S. Liu, 'Effects of different thermal conductivity enhancers on the thermal performance of two organic phase- change materials: paraffin wax RT42 and RT25', *J. Enhanc. Heat Transf.*, vol. 20, no. 6, 2013.

[9] M. Fuensanta, *et al.*, 'Thermal properties of a novel nanoencapsulated phase change material for thermal energy storage', *Thermochim. Acta*, pp. 95–101, Aug. 2013.

[10] X. Jia *et al.*, 'High thermal conductive shape-stabilized phase change materials of polyethylene glycol/boron nitride@chitosan composites for thermal energy storage', *Compos. Part Appl. Sci. Manuf.*, vol. 129, p. 105710, Feb. 2020.

[11] T. Qian, *et al.*, 'Enhanced thermal conductivity of PEG/diatomite shape-stabilized phase change materials with Ag nanoparticles for thermal energy storage', *J. Mater. Chem. A*, vol. 3, no. 16, pp. 8526–8536, Apr. 2015.

[12] Y. Lin, *et al.*, 'Review on thermal conductivity enhancement, thermal properties and applications of phase change materials in thermal energy storage', *Renew. Sustain. Energy Rev.*, vol. 82, pp. 2730–2742, Feb. 2018.

[13] C. Ho, *et al.*, 'Efficacy of turbulent convective heat transfer in a circular tube with water-based nanoemulsion of n–Eicosane–An experimental study', *Int. J. Heat Mass Transf.*, vol. 183, p. 122062, Feb. 2022.

[14] M. S. Shafiq, M. M. Khan, and M. Irfan, 'Performance enhancement of double-wall-heated rectangular latent thermal energy storage unit through effective design of fins', *Case Stud. Therm. Eng.*, vol. 27, Oct. 2021.

[15] A. Sciacovelli and V. Verda, 'Second-law design of a latent heat thermal energy storage with branched fins', *Int. J. Numer. Methods Heat Fluid Flow*, vol. 26, no. 2, pp. 489–503, Jan. 2016.

[16] T. Barz *et al.*, 'Experimental Analysis and Numerical Modeling of a Shell and Tube Heat Storage Unit with Phase Change Materials', *Ind. Eng. Chem. Res.*, vol. 55, no. 29, pp. 8154–8164, Jul. 2016.

[17] M. K. Koukou *et al.*, 'Experimental assessment of a full scale prototype thermal energy storage tank using paraffin for space heating application', *Int. J. Thermofluids*, vol. 1–2, p. 100003, Feb. 2020.

[18] K. D'Avignon and M. Kummert, 'Experimental assessment of a phase change material storage tank', *Appl. Therm. Eng.*, vol. 99, pp. 880–891, Apr. 2016.

[19] M. S. Mahdi, *et al.*, 'Numerical simulations and experimental verification of the thermal performance of phase change materials in a tube-bundle latent heat thermal energy storage system', *Appl. Therm. Eng.*, vol. 194, p. 117079, Jul. 2021.

[20] J. Tombrink, H. Jockenhöfer, and D. Bauer, 'Experimental investigation of a rotating drum heat exchanger for latent heat storage', *Appl. Therm. Eng.*, vol. 183, p. 116221, Jan. 2021, doi: 10.1016/j.applthermaleng.2020.116221.

[21] Y. Maleki, M. Mehrpooya, and F. Pourfayaz, 'Cold thermal energy storage by encapsulated phase change materials system using hybrid nanofluids as the heat transfer fluid', *Int. J. Energy Res.*, vol. 45, no. 10, pp. 15265–15283, 2021.

[22] D. Chen, *et al.*, 'Numerical investigation on performance improvement of latent heat exchanger with sextant helical baffles', *Int. J. Heat Mass Transf.*, vol. 178, p. 121606, Oct. 2021.

[23] 'Organic Phase Change material: Tempered entropy', Innovative China Leading PCM Company. Accessed on: Nov. 27, 2021. Available: https://www.pcmgel.com.

[24] 'Programmable Resolution 1-Wire Digital Thermometer', Digi-Key Electronics, Minnesota, USA. Accessed on: Nov. 27, 2021. Available https://www.digikey.co.uk.

[25] 'Single Jet Flow Water Meter Technical Data', Meters UK Ltd, Lancaster, UK. Accessed on: Nov. 27, 2021. Available: https://meters.co.uk.

[26] 'Water flow sensor YF-S201 Flowmeter', URUK, Baghdad, Irak, Accessed on: Nov. 27, 2021. Available: https://www.uruktech.com/.

[27] 'Willis External Immersion Heater Technical Data', Willis heating & plumbing company Ltd, Belfast, UK. Accessed on: Nov. 27, 2021. Available: https://willis-heating.com.

[28] 'Sonoff BasicR2/RFR2', Sonoff, Shenzhen, GD. Accessed on: Dec. 02, 2021. Available: https://sonoff.tech/.

[29] 'UPS3 Central Heating Circulator Data Sheet', Grundfos A/S, Bjerringbro, Denmark. Accessed on: Nov. 27, 2021. Available: https://www.grundfos.com/.

[30] 'Parker Chemical Hose Tube Materials', Parker Hannifin Corp, Cleveland, USA. Accessed on: Nov. 27, 2021. Available: https://www.parker.com.

[31] 'Product overview, insulation Technical Data', NMC, Eynatten, Belgium. Accessed on: Dec. 15, 2021. Available: https://nmc-insulation.com.

[32] 'Pegler Peg402 TMV Valve Technical Data', Pegler Yorkshire Ltd, Doncaster, Yorkshire, UK. Accessed on: Nov. 27, 2021. Available: https://www.pegleryorkshire.co.uk